Reprinted from

thin solid films

Thin Solid Films 307 (1997) 106–109

A model of oxide layer growth on Ag^+ and Pt^+ ion implanted nickel anode in aqueous alkaline solution

I.S. Tashlykov *

Belorussian State Technological University, 13-a Sverdlova Str., 220630 Minsk, Belarus

Received 9 October 1996; accepted 17 April 1997

ELSEVIER

ELSEVIER

Thin Solid Films 307 (1997) 106–109

thin solid films

A model of oxide layer growth on Ag^+ and Pt^+ ion implanted nickel anode in aqueous alkaline solution

I.S. Tashlykov *

Belorussian State Technological University, 13-a Sverdlova Str., 220630 Minsk, Belarus

Received 9 October 1996; accepted 17 April 1997

Abstract

This work investigates nickel oxide films growth on nickel implanted with ions of the noble metals Ag and Pt. Polycrystalline and single crystal samples of Ni were implanted with high fluences (1×10^{19}–1×10^{21} m^{-2}) of 9–50 keV ions. Galvanostatic and potentiostatic polarization techniques were applied to monitor the electrochemical efficiencies of formation of Ni_XO_{1-X} films in aqueous KOH solution (30%) at 353 K. The growth rates, thickness and compositional profiles of oxidised nickel layers were examined by means of RBS. It was found that the anodic oxide film consists of $Ni(OH)_2 X H_2O$ ($X \geq 1$). Anodic oxidation of nickel occurs due to out-diffusion of Ni atoms through the hydroxide layer. Implanted Ag penetrates partly into the anodic oxide whereas platinum is completely buried beneath the oxide film. © 1997 Elsevier Science S.A.

Keywords: Oxide growth; Nickel; Ion implantation; RBS

1. Introduction

Nickel, as is known, possesses high corrosion resistance in aqueous alkaline solutions and simultaneously has a sufficiently high electrocatalytic activity for the oxygen liberation reaction from such solutions. Consequently, nickel is widely used as a material for anode fabrication in commercial electrolyses. There are several publications [1–4] describing attempts to improve the nickel electrode efficiency by means of ion implantation. However, the properties of nickel oxides which usually cover ion-implanted oxygen electrodes have not been discussed, in spite of the fact that at a potential higher than +0.2 V (relative to the hydrogen electrode) the oxygen evolution always emanates at the oxidised nickel [5]. Therefore, the electrochemical properties of such electrodes depend very sensitively on the behaviour of the surface oxide film on the anode [6–8]. For this reason, there is a considerable interest in the mechanisms of oxide growth on ion-implanted nickel and in studying the changes in composition of the surface layers as a function of the implanted species.

In the present investigation, we have studied the surface of Ni and the oxidation after implantation with silver and platinum ions and subsequently used these as anodes for electrolytes in aqueous alkaline solutions. Silver and platinum were chosen for ion implantation because of their well-known electrocatalytic performance and stability in alkaline solutions. Additionally, it is known that silver is insoluble in nickel, in contrast to platinum which creates a solid solution with nickel at all concentrations [9]. Therefore, one could expect different behaviours of the implanted species during oxidation of nickel in the electrolyte. It is known that silver ions precipitate in nickel when implantation doses are larger then 1×10^{20} m^{-2} [4,10]. For this reason, we used the silver peak as a marker for investigation of the thin oxide film growth mechanism at anodic oxidation of ion implanted nickel in aqueous alkaline solution.

2. Experimental procedure

Poly- and single-crystal samples of Ni with diameter 10 mm were implanted with 9, 40 and 50 keV Ag^+ and Pt^+ ions at room temperature with fluences in the range 1×10^{19}–1.1×10^{21} m^{-2}. The scanned beam current was varied between 7 mA m^{-2} and 25 mA m^{-2} for different sets of experiments.

* Corresponding author.

PII S0040-6090(97)00227-7

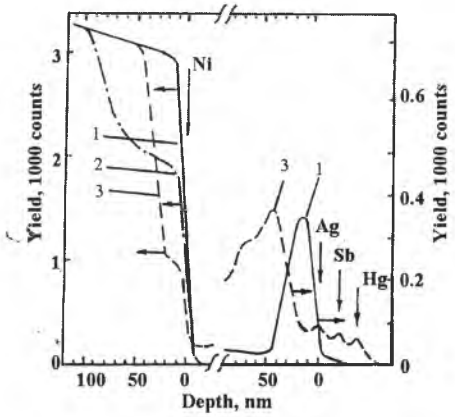

Fig. 1. RBS spectra of 2 MeV He ($\Theta = 150°$, entry and escape angles are $\Theta_1 = O°$, $\Theta_2 = 30°$) for Ni polycrystals: 1-implanted with 50 keV Ag^+ ions, dose 2×10^{20} m^{-2}; 2-thermally oxidized Ni; 3-sample 1 after anodic polarization (sample is tilted to 65°).

Steady-state anodic polarisation measurements were made in a teflon cell which has previously been described in detail [1] in 30% KOH solutions at a temperature of 383 K as electrolyte. The sample anode potential was measured vs. a Pt dynamic hydrogen reference electrode, described previously [11] over a wide range of current densities (1–20 kA m^{-2}). Backscattering of 0.5, 0.7 and 2.0 MeV He^4 with a scattering angle (Θ) of 150° and 168° was used to study the composition of the resulting surface layers. To improve the depth resolution of the system, some of the samples were tilted by 60–70° to the incident beam providing a total depth resolution of ≈ 8 nm for nickel. Thus, depth scale, rather than, channel number scale is shown for a comparison of the RBS spectra in Fig. 1. Several experiments were conducted using an electrostatic analyser (ESA) and approximately 1 nm depth resolution (Δt) of the analysing system for nickel was achieved. Ni samples thermally oxidized in air at $T = 723$ K, were used in order to produce a film of NiO at the surface as demonstrated by Graham and Cohen [12]. Bragg's rule was applied for composition analysis of the oxidized nickel films.

3. Results and discussion

The composition of the oxide film on thermally oxidized nickel as analysed by RBS is shown as curve 2 in Fig. 1 and coincides with the expected curve for NiO. The thickness of the NiO layer is 40–45 nm and agrees with an estimate from Graham and Cohen [12], for which the oxidation time was 20 min. There was no apparent deviation from Bragg's rule for the Ni–O system.

Ion implantation of Ag into nickel leads to a significant reduction in the total overpotential. This result was first observed by Acano et al. [1] and later confirmed by Tashlykov et al. [4] and is consistent with the observation by Shumilova and Zutaeva [13] that the measured nickel activity in the oxygen evolution reaction is increased when silver is thermally inserted into nickel from a silver–nickel powder at high temperature. Experimental data about the influence of silver ion implantation into nickel on activity of the Ni anode during electrolysis are presented in Table 1. In a region of low (1 kA m^{-2}) current density, the overpotential of oxygen evolution when modified anodes are used is 320–340 mV less than in virgin nickel anode application. When current density of an electrolysis process is 10 kA m^{-2}, an observable overpotential is reduced compared with that of the unimplanted electrode by the amount from 250–360 mV. Some decrease of the modified electrodes activity when doses of Ag^+ ions are more than 10^{20} m^{-2} may be explained by the precipitation of silver, which was observed in ion-implanted nickel by means of TEM (polycrystals) and RBS/Channelling (single crystals) using measurements of energy dependence of He^+ ions dechannelling rate [10,14]. In the investigated range of implantation energies, there was no noticeable effect of ion energy on an anode activity observed. This fact may mean that at the circumstances of our study there was always enough silver atoms to provide necessary electroconductivity of nickel oxide layer on anode surface.

The RBS spectra, shown in curves 1 and 3 in Fig. 1, represent the general features of the oxide formation on the surface of the Ag^+ ion implanted nickel during anodic oxidation. We consider that in nickel oxide growth by only anion migration, one should observe the growth of oxide layer (appearance of a step in the region of nickel signal) and approximately unchanged position of silver peak in energetic RBS spectrum. When both cation and anion migration takes place during nickel oxide growth, one should observe, additionally to appearance of the step, slight movement of the silver front edge to the low energy direction in the RBS spectrum. We observed a correlation of the oxide layer thickness with depth of the silver signal shift to the left. This behaviour of signals in RBS spectra of all investigated samples allows us to suggest the proposed model of nickel oxide growth by cation migration alone in the present study. The step on spectrum 3 in Fig. 1 is interpreted as a result of oxide creation with compositions that fit to the formula of $Ni(OH)_2 X H_2O$ ($X \geq 1$). This result differs very significantly from the content of the Ni surface after thermal oxidation, but agrees with the data of Ivanova et al. [15], where the composition of the nickel electrode in a 5N KOH electrolyte was investigated and Kowal et al. [16], who studied the Ni electrode by in

Table 1
Total overpotential measured during electrolysis using 50 keV Ag^+ ion-implanted nickel anodes

	Layer conc. [a]	0	2.8	8.7	10	29
Overpotential, V	1 kA m^{-2}	0.70	0.36	0.38	0.38	0.38
At current density	10 kA m^{-2}	0.80	0.49	0.44	0.53	0.55

[a] of silver implanted into nickel, 1×10^{19} m^{-2}.

situ atomic force microscopy. It was obtained in our experiment that the thickness of the hydroxide layers on Ag^+ ion-implanted nickel does not depend significantly on the dose of ions and is in the range 30–50 nm. This experimentally measured thickness of oxide nickel layer is many times bigger than discussed in Ref. [6] but almost the same as was observed by Thompson et al. [2]. No growth of the oxide thickness with increasing polarization time was observed. The correlation of the oxide layer thickness with depth of the Ag peak shift, shown in curves 1 and 3 at the left and right hand side of Fig. 1, indicates that the oxidation of the Ag^+ ion-implanted nickel is caused by migration of cation towards the surface during anodic film formation, as also occurring during thermal oxidation of nickel [17,18]. This suggests a model in which the host atoms undergo replacements under the influence of a very high electric field. However, in contrast to the data [19,20] on the transport of both anions and cations during anodic oxidation of Al, Nb, Ta and W and oxygen migration alone into Zr and Hf, no diffusion of oxygen into nickel was observed. The spectra 1 and 3 in Fig. 1 are noteworthy in the fact that during anodic oxidation, Ag atoms are expected to be mobile in nickel oxide. A 'tail' of the silver in Fig. 1, curve 3, shows that Ag is present in the oxide film at a concentration of about 2% at the surface. This result was checked precisely using an ESA for RBS measurements at the Max Planck Institute for Nuclear Physics in Heidelberg. One can see a few extra peaks shown by curve 3 in Fig. 1, which were observed every time after electrochemical treatments. They are associated with the presence on the surface of the oxide of small amounts ($< 1 \times 10^{18}$ m^{-2}) of heavy elements, probably Sb and Hg, which may be in the electrolyte as noncontrolled impurities.

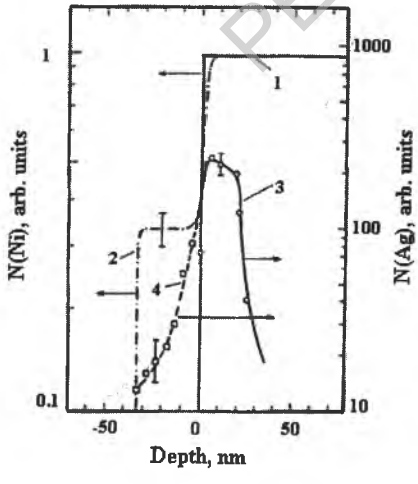

Fig. 2. Derived from RBS spectra elemental depth profiles in Ni single crystal implanted with Ag^+ ions ($E = 40$ keV, dose 1.4×10^{20} m^{-2}): 1-Ni, 3-Ag ($\Delta t = 4.6$ nm), after anodic polarization 2-Ni, 4-Ag ($\Delta t = 1$ nm, the spectrum was taken using ESA). Depth scale with sign '−' is applied to show the growth of the oxide layer by outward cations migration during electrolysis.

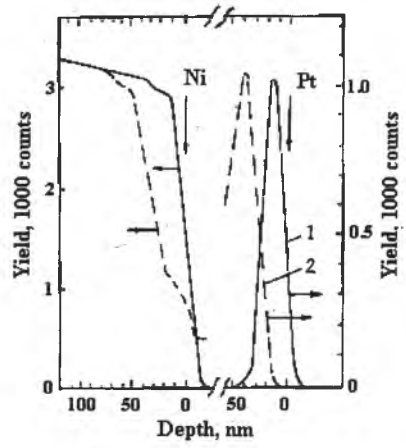

Fig. 3. RBS spectra of 2 MeV He ($\Theta = 150°$, tilt angle 65°) for Ni: 1-implanted with 50 keV Pt^+ ions, dose 2.3×10^{20} m^{-2}, 2-after anodic polarization.

A comparison of the calculated experimental RBS spectra of the 40 keV Ag^+ implanted and electrolytically oxidized nickel is given in Fig. 2. Curve 2 in Fig. 2 indicates that the content of the surface oxide corresponds to the formula NiO(OH). The presence of silver in the oxide film, (curve 4 in Fig. 2) is clearly evident. This suggests a model in which a portion of the implanted Ag atoms follow the nickel atoms in their out-diffusion during anodic oxidation. Such behaviour of silver atoms may explain the increase in the energy efficiency of electrolysis when Ag^+ ion implanted anodes are used [1–4].

The electrocatalytic properties of Pt^+ ion implanted nickel differ from the activity of virgin nickel anodes only at a first stage of electrolysis. A few minutes after the beginning of the process, this property of the modified anode drops up to pure nickel anode activity. RBS spectra, which are presented in Fig. 3, demonstrate one of the possible reasons for this phenomenon. An appearance of a step on spectrum 2 in Fig. 3, the thickness of which is equal to the shift of the Pt peak to the left hand side, are very similar to the changes of the spectra in Fig. 1. This suggests a process in which the growth of the hydroxide film on Pt^+ ion implanted Ni during electrolysis can be attributed to out-diffusion of cations. The absence of Pt in the near surface region of the oxidized film indicates that implanted Pt atoms are buried beneath the oxide film, and therefore do not influence the energy efficiency of electrodes [3].

Calculations of the Pt peak after implantation and after polarization experiments show that there is very small decrease in the platinum content indicating that this proposal is correct. On the other hand, we observed a 6–11% loss of Ag in the polarisation measurements that were performed with electrodes implanted with different doses of Ag^+ ions as shown in Table 2. The energies of Ag^+ and Pt^+ ions in the interval investigated did not play an

Table 2
Content of ion-implanted species in nickel anode before and after polarization

Ion	E (keV)	Layer concentration (m^{-2})	
		As implanted	After polarization
Pt	9	3.0×10^{19}	2.9×10^{19}
	50	2.3×10^{20}	2.3×10^{20}
Ag	40	1.4×10^{20}	1.3×10^{20}
	50	2.8×10^{19}	2.5×10^{19}
		8.7×10^{19}	7.8×10^{19}
		2.9×10^{20}	2.7×10^{20}

important role in the mechanism of nickel oxidation in an aqueous alkaline solution.

4. Conclusion

Ion implantation was employed to introduce silver and platinum into nickel anodes to study electrolysis in H_2O. RBS analysis of the oxidized nickel showed that electrolysis is associated with out-diffusion of Ni atoms through the hydroxide film. Implanted Ag partly penetrates into the anodic oxide, whereas Pt is completely buried beneath the oxide film. Such behaviour of Ag atoms suggests a model where they follow the nickel atoms as they out-diffuse during anodic oxidation. This is one of the effects related to the insolubility of Ag in nickel. Mechanisms of oxidation of Ag^+ and Pt^+ ion-implanted Ni did not appear to be sensitively dependent on ion dose and energy in the intervals investigated. The content of the anodic oxide corresponds to the formula $Ni(OH)_2\,X\,H_2O$ ($X \geq 1$).

Acknowledgements

A portion of this work was performed at McMaster and Salford Universities and at M.P. Institute for Nuclear Physics. The sponsorship of the Royal Society of Great Britain and Deutscher Akademischer Austauschdienst (Contract 325-96mj) is gratefully acknowledged.

References

[1] U. Acano, J.A. Davies, W. Smeltzer, I.S. Tashlykov, D.A. Thompson, Nucl. Instr. and Meth. 182–183 (1981) 985.
[2] D.A. Thompson, U. Acano, J.A. Davies, W. Smeltzer, Proc. 3rd Int. Conf. Modification Surface Properties of Metals by Ion Implantation, Oxford, 1982, p. 46.
[3] J.A. Davies, I.S. Tashlykov, D.A. Thompson, Trudy XI Vses. Sovesch. po Phys. Vzaimodeistvija Zarjazhennykh Chastits s Crystallami, Moscow, 1982, p. 417 (in Russian).
[4] I.S. Tashlykov, E.B. Boiko, O.A. Slesarenko, F.F. Komarov, Phys. and Chem. of Materials Treatment 6 (1986) 9, (in Russian).
[5] M.A. Dasojan, Khimicheskie istochniki toka, Leningrad, 1969 (in Russian).
[6] L.M. Elina, T.I. Borisova, C.I. Zalkind, J. Phys. Chem. 28 (1954) 785, (in Russian).
[7] W.-H. Zhu, J.-J. Ke, H.-M. Yu, D.-J. Zhang, J. Power Source 56 (1995) 75.
[8] J. Niedbala, A. Budniok, G. Gierlotka, J. Surowka, P. Matyja, Thin Solid Films 266 (1995) 113.
[9] E.M. Savitski (Ed.), Blagorodnye metally, Moscow, 1984 (in Russian).
[10] P. Wang, D.A. Thompson, W. Smeltzer, Nucl. Instr. and Meth. (in Physics Research) B7–8 (1985) 97.
[11] J. Giner, J. Electrochem. Soc. 111 (1964) 376.
[12] M.J. Graham, M.J. Cohen, J. Electrochem. Soc. 119 (1972) 879.
[13] N.A. Shumilova, G.V. Zutaeva, Toplivnye Elementy, Kinetika Electrodnykh Processov, Moscow, 1968, p. 138 (in Russian).
[14] I.S. Tashlykov, Z. Al-Tamimi, Surface Phys. Chem. Mechanics 7 (1991) 145, (in Russian).
[15] A.M. Ivanova, L.A. Salnikov, L.P. Timofeeva, L.O. Favorskaja, Electrochimija 21 (1985) 1287, (in Russian).
[16] A. Kowal, R. Niewiara, B. Peronczyk, J. Haber, Acta Phys. Pol. A 89 (3) (1996) 401.
[17] P. Kofstad, Proc. JIMIS-3 (1983) High Temperature Corrosion Transactions of the Japan Institute of Metals (Suppl.), Tokyo, 1983, p. 1.
[18] Z. Rao, J.S.W. Williams, D.K. Sood, Surf. Coat. Technol. 51 (1992) 52.
[19] J.A. Davies, B. Domeij, J.P.S. Pringle, F. Brown, J. Electrochem. Soc. 112 (1965) 675.
[20] J. Perriere, J. Sijeka, S. Rigo, Corr. Sci. 20 (1980) 91.